MATHEMATICAL BIOSCIENCES
AND ENGINEERING
Volume **8**, Number **2**, April **2011**

doi:10.3934/mbe.2011.8.371

pp. **371–383**

TUMOR CELLS PROLIFERATION AND MIGRATION UNDER THE INFLUENCE OF THEIR MICROENVIRONMENT

Avner Friedman

Department of Mathematics
Ohio State University
Columbus, OH 43210, USA

Yangjin Kim

Department of Mathematics and Statistics
University of Michigan
Dearborn, MI 48128, USA

Abstract. It is well known that tumor microenvironment affects tumor growth and metastasis: Tumor cells may proliferate at different rates and migrate in different patterns depending on the microenvironment in which they are embedded. There is a huge literature that deals with mathematical models of tumor growth and proliferation, in both the avascular and vascular phases. In particular, a review of the literature of avascular tumor growth (up to 2006) can be found in Lolas [8] (G. Lolas, Lecture Notes in Mathematics, Springer Berlin / Heidelberg, 1872, 77 (2006)). In this article we report on some of our recent work. We consider two aspects, proliferation and of migration, and describe mathematical models based on *in vitro* experiments. Simulations of the models are in agreement with experimental results. The models can be used to generate hypotheses regarding the development of drugs which will confine tumor growth.

1. **Tumor cells and fibroblasts in a transwell.** Significant evidence exists that fibroblasts and myofibroblasts residing in the tumor microenvironment affect tumor cell proliferation. Recently, Samoszuk *et al.* [11] demonstrated the ability of fibroblasts to enhance the growth of a relatively small number of breast cancer cells *in vitro*. Yashiro *et al.* [17] also demonstrated that tumor size is significantly increased in mice when breast cancer cells are co-inoculated with breast fibroblasts. In other experiments it was shown that fibroblasts cultured from normal tissue tend to have inhibitory effects on cell growth, whereas fibroblasts cultured from tumors stimulate the growth of several cell types, including muscle cells, mammary carcinoma cells and myofibroblasts [3, 9]. A transwell kit that is used to explore tumor cells proliferation under the influence of fibroblasts is shown in Figure 1. The interaction between the TECs and the fibroblasts is mediated by cytokines, namely, by epidermal growth factors (EGFs) produced by the TECs and transformed growth factor-β (TGF-β) produced by the fibroblasts. During a period of several days a large number of fibroblasts differentiate into myofibroblasts which secrete EGF at larger rates than fibroblasts. The cytokines can cross the membrane, but the cells

2000 *Mathematics Subject Classification.* Primary: 92C45, 92C50; Secondary: 92B05.

Key words and phrases. Cancer, tumor growth, microenvironment.

The authors are supported by NSF/DMS upon agreement 112050. Yangjin Kim was supported by a Rackham grant from the Horace H. Rackham School of Graduate Studies, University of Michigan.

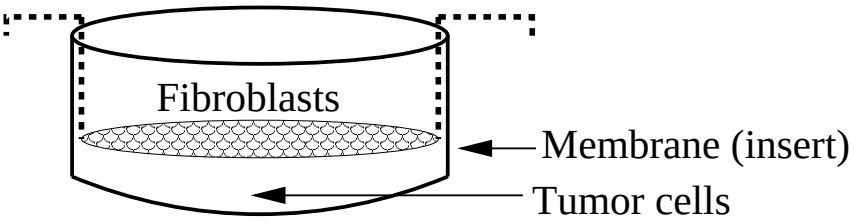

FIGURE 1. Structure of a transwell kit. Tumor epithelial cells (TECs) are deposited in the lower chamber and fibroblasts are deposited in the upper chamber. The two chambers are separated by a semi-permeable membrane.

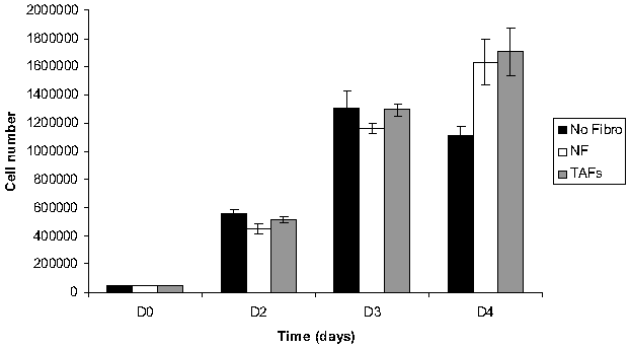

FIGURE 2. Growth of epithelial F-305 cells plated with no fibroblasts, normal mammary fibroblasts or tumorigenic mammary fibroblasts. Cells were initially plated at a 1:6 ratio of fibroblasts to epithelial cells and then counted on days 2, 3 and 4. *NF* normal fibroblasts, *TAFs* tumor associated fibroblasts.

cannot cross it. Figure 3 shows a schematic of the interaction between the cells and cytokines in a simple 2-d geometry.

Experiments were conducted by Kim *et al.* [6] using two kinds of fibroblasts: normal mammary fibroblasts and tumorigenic mammary fibroblasts. The results of the experiments are shown in Figure 2. It was demonstrated that in the presence of tumorigenic fibroblasts, the TECs proliferated at a larger rate. A mathematical model, developed in [6], is based on the simplified 2D geometry of Figure 3. It includes the following functions:

$$
\begin{aligned}
n &= \text{density of TEC},\\
f &= \text{density of fibroblast},\\
m &= \text{density of myofibroblast},\\
E &= \text{concentration of EGF, and}\\
G &= \text{concentration of TGF-}\beta.
\end{aligned}
$$

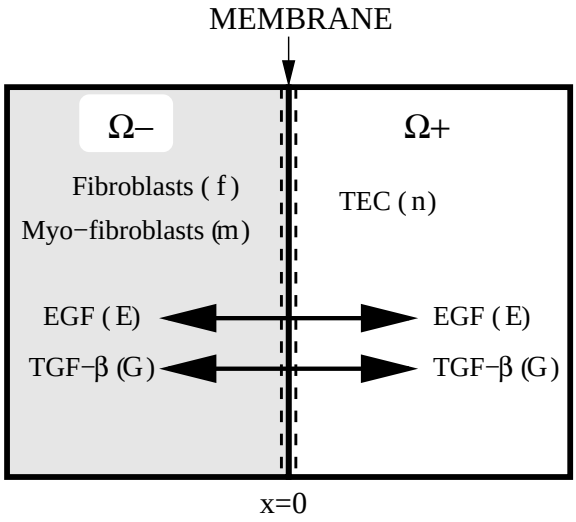

FIGURE 3. Schematics of the interactions across the membrane. While EGF and TGF-β can move across the semi-permeable membrane, tumor cells, fibroblasts, and myofibroblasts cannot cross the membrane.

Ignoring the vertical variable in Figure 3, these functions satisfy a system of partial differential equations in (x,t):

$$\frac{\partial n}{\partial t} = \underbrace{\frac{\partial}{\partial x}\left(D_n \frac{\partial n}{\partial x}\right)}_{\text{Random walk}} - \underbrace{\frac{\partial}{\partial x}\left(\chi_n\, n\, \frac{\frac{\partial E}{\partial x}}{\sqrt{1+(\frac{\partial E}{\partial x}/\lambda_E)^2}}\right)}_{\text{Chemotaxis}}$$
$$+ \underbrace{a_{11}\, \frac{E^4}{k_E^4+E^4}\, n(1-n/\kappa)}_{\text{Proliferation}},\ 0<x<L/2, \tag{1}$$

$$\frac{\partial f}{\partial t} = \underbrace{\frac{\partial}{\partial x}\left(D_f \frac{\partial f}{\partial x}\right)}_{\text{Random walk}} - \underbrace{a_{21}\, G\, f}_{f\to m} + \underbrace{a_{22} f}_{\text{Proliferation}},\ -L/2<x<0, \tag{2}$$

$$\frac{\partial m}{\partial t} = \underbrace{\frac{\partial}{\partial x}\left(D_m \frac{\partial m}{\partial x}\right)}_{\text{Random walk}} - \underbrace{\frac{\partial}{\partial x}\left(\chi_m\, m\, \frac{\frac{\partial G}{\partial x}}{\sqrt{1+(\frac{\partial G}{\partial x}/\lambda_G)^2}}\right)}_{\text{Chemotaxis}} + \underbrace{a_{21}\, G\, f}_{f\to m}$$
$$+ \underbrace{a_{31}\, m}_{\text{Proliferation}},\ -L/2<x<0, \tag{3}$$

$$\frac{\partial E}{\partial t} = \underbrace{\frac{\partial}{\partial x}\left(D_E \frac{\partial E}{\partial x}\right)}_{\text{Diffusion}} + \underbrace{(a_{41}\, f + B a_{41}\, m)}_{\text{Production}} - \underbrace{a_{43}\, E}_{\text{Decay}},$$
$$-L/2<x<L/2, \tag{4}$$

$$\frac{\partial G}{\partial t} = \underbrace{\frac{\partial}{\partial x}\left(D_G \frac{\partial G}{\partial x}\right)}_{\text{Diffusion}} + \underbrace{a_{51}\, n}_{\text{Production}} - \underbrace{a_{52}\, G}_{\text{Decay}},\ -L/2<x<L/2. \tag{5}$$

All the concentrations in equations (1)-(5) include a diffusion term. Equation (4) includes production of EGF by fibroblasts and myofibroblasts , and a degradation term. Equation (5) include production of TGF-β by TECs and a degradation term. The second term in equation (1) expresses the fact that TECs are attracted in the direction of concentration gradient of EGF (chemotaxis) and, similarly, equation (3) includes the chemotactic attraction of myofibroblasts in the direction of the concentration gradient of TGF-β. The last term on the right-hand side of equation (1) is a logistic growth of the density of TECs enhanced by EGF by a factor which was derived from experimental measurement. Equation (2) includes proliferation of fibroblasts and a term expressing the transformation of fibroblasts to myofibroblasts under the influence of TGF-β.

The fact that the semi-permeable membrane allows EGF and TGF-β to cross over, but not cells, is represented mathematically by the following boundary conditions at the membrane x=0:

$$(D_n\nabla n - \chi_n n\frac{\nabla E}{\sqrt{1+(|\nabla E|/\lambda_E)^2}})\cdot\nu = 0 \quad \text{at } x=0+, \tag{6}$$

$$D_f\nabla f\cdot\nu = 0,\ (D_m\nabla m - \chi_m m\frac{\nabla G}{\sqrt{1+(|\nabla G|/\lambda_G)^2}})\cdot\nu = 0 \quad \text{at } x=0-,$$

and

$$\frac{\partial E^+}{\partial x} = \frac{\partial E^-}{\partial x},\ -\frac{\partial E^+}{\partial x} + \gamma(E^+ - E^-) = 0, \tag{7}$$

$$\frac{\partial G^+}{\partial x} = \frac{\partial G^-}{\partial x},\ -\frac{\partial G^+}{\partial x} + \gamma(G^+ - G^-) = 0,$$

where

$$E(x) = \begin{cases} E^+(x) & \text{if } x>0 \\ E^-(x) & \text{if } x<0 \end{cases},\ G(x) = \begin{cases} G^+(x) & \text{if } x>0 \\ G^-(x) & \text{if } x<0 \end{cases},$$

ν is the outward normal, and γ is a positive parameter which is determined by the size and density of the holes in the membrane.

Figure 4 shows simulation of the model, where the cell density in the model was interpreted (by introducing a proportionality factor) as cell number. The simulation results are in good agreement with the experimental results, marked by squares. The statistical goodness of fit by the model was confirmed by strong positive correlation coefficient (=0.993) between the experimental data and simulation results. Since only four measurements were done to obtain each experimental data point, each data point exhibited in Figure 4 was taken as the means of the four measurements.

2. **Tumor cells and fibroblasts in invasion assay system.** Invasion assay systems are used to study the influence of chemotactic and haptotactic forces on tumor cells. Figure 5 illustrates a Boyden chamber invasion assay that mimics tumor invasion *in vivo* [18]. A semi-permeable membrane separating the two chambers is coated with gel, or extracellular matrix (ECM), in order to represent *in vivo* situation of the basal membrane in mammary gland, for instance.

The mathematical model which describes tumor cells proliferation and migration now includes, in addition to the variables introduced in Section 1, also Matrix Metalloproteinase (MMP) secreted by the fibroblasts and myofibroblasts, and the ECM density. The model developed by Kim and Friedman [5] is based on the

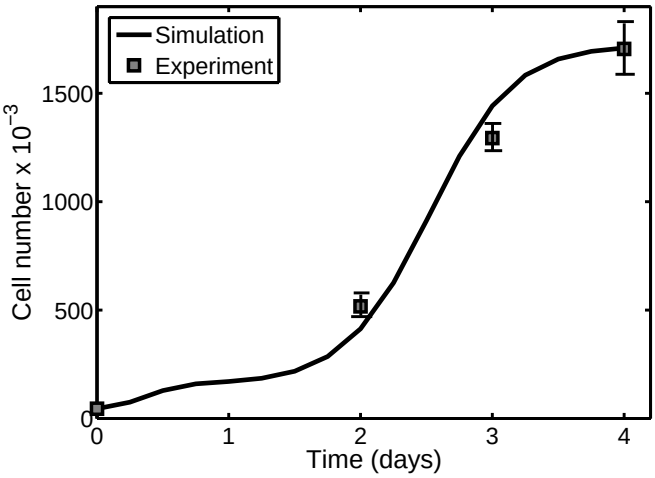

FIGURE 4. (a) Simulation results at day 4. Comparison of simulation results (solid curve) to experimental results (marked by squares) for F305 cell line. The correlation coefficient between the experimental data and simulation results is 0.9931.

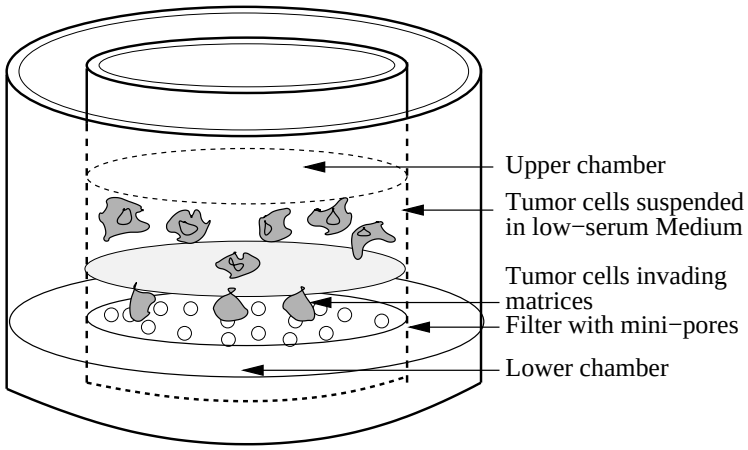

FIGURE 5. Illustration of a Boyden Chamber Invasion Assay that mimics tumor invasion *in vivo*

geometry shown in Figure 6. The ECM, which is degraded by the TECs, gives rise to haptotaxis; chemotaxis arises from the gradient of the EGF and TGF-β. The mathematical model has also been extended, in [5], to the case where the membrane is permeable to cells.

Simulations of the model yield some interesting results:
(i) Figure 7(a) shows that when cells cannot cross the membrane, the TEC population (in the right chamber) has a biphasic dependence on the concentration of the gel.

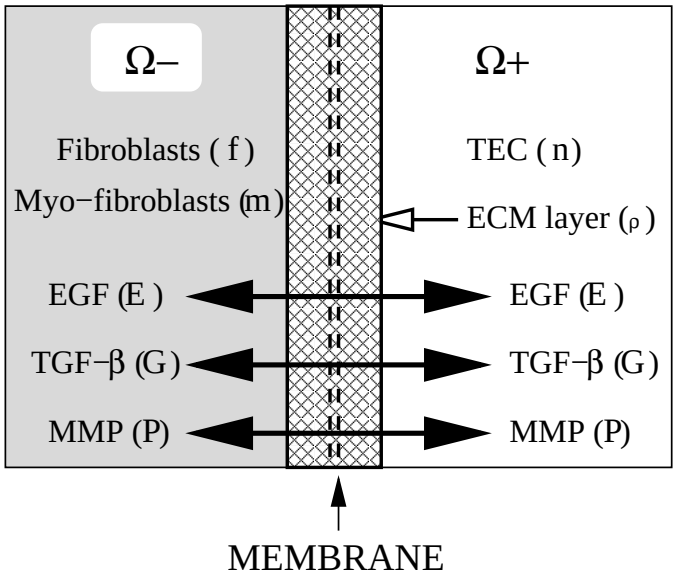

FIGURE 6. Schematics of an Invasion Assay System : EGF (E), TGF-β (G) and MMP (P) can cross the semi-permeable membrane, but the cells (TECs (n), fibroblasts (f), myofibroblasts (m)) may not cross it. Initially the TECs reside in the domain Ω_+ while fibroblasts and myofibroblasts are placed in the domain Ω_-. An ECM layer surrounds the semi-permeable membrane (filter).

Figure 7(b) shows that when cells can cross the membrane and thus invade the left chamber, if the ECM concentration is increased in the left chamber Ω_-, then the population of TECs in the left chamber will increase. These simulation results are in qualitative agreement with experimental measurements reported in [2, 10, 13].

(ii) If we denote the width of the ECM layer by μ, then the total population of TECs is a decreasing function of μ for $\mu < \mu_0$ and an increasing function of μ for $\mu > \mu_0$, as shown in Figure 8 (Here cells can cross the membrane). One possible explanation of the above behavior is as follows: If μ increases, the haptotactic forces increase, causing TECs to move faster toward the membrane. However, within the ECM there is competition for space, so that tumor cells cannot proliferate as fast as those outside the ECM. As a result of this competition the TEC population decreases as μ is increased, but only as long as μ remains smaller than μ_0. When μ becomes larger than μ_0, the chemotactic forces (which depend on the proximity of the TECs to fibroblasts/myofibroblasts) increase to the extend that they more than compensate for the reduced proliferation caused by the "competition for space;" hence the total population of TEC increases with μ when $\mu > \mu_0$. It would be interesting to test the conclusions of the above simulations experimentally.

The mathematical model can be used to make hypotheses regarding drugs that will block tumor growth. The model predicts that a drug which blocks the production of MMP by fibroblasts/myofibroblasts or the MMP activity will slow down tumor growth, as seen in Figure 9.

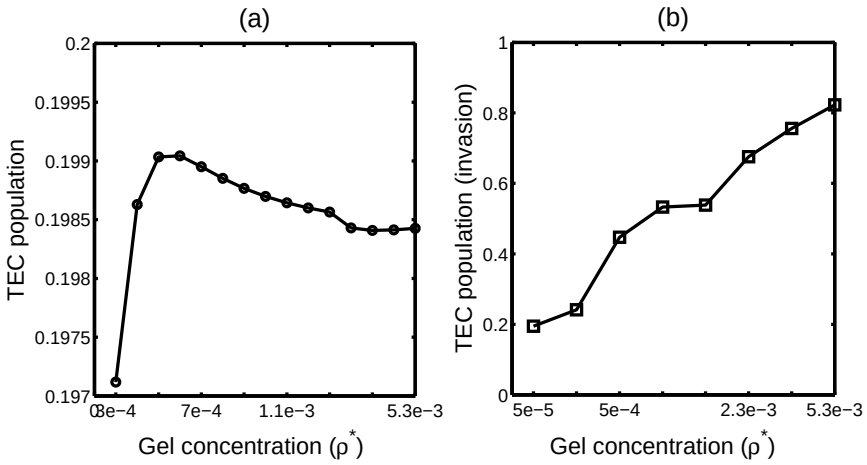

FIGURE 7. (a) Bifurcation diagram showing how total TEC population at $t = 13h$ depends on the gel concentration ρ^*. Biphasic dependence of the TEC population is seen. (b) Effect of gel concentration on TEC invasion: Total TEC population in the left chamber for different gel concentration in the left chamber and fixed gel concentration in the right chamber. As the gel concentration increases, the TEC population in the left chamber increases.

Another strategy to stop or slow down tumor growth is to block the production of TGF-β by TECs. Figure 10 shows that proliferation and invasion are reduced by this procedure. The predictions described by Figures 9 and 10 need to be validated experimentally.

3. **Patterns of migration.** In Section 2 we considered the chemotactic and haptotactic effects on tumor cell migration when these cells are placed in one compartment of an invasion assay. In this section we consider the migration *pattern* of tumor cells, rather than the *number* of migrating cells. This migration pattern again depends on the type of cells and on the tumor environment. Knowing the pattern of cell migration is important for predicting metastasis. This is particularly important in the case of an aggressive cancer like glioblastoma. A major reason for treatment failure of glioblastoma is that by the time the disease is diagnosed tumor cells have already migrated from the primary tumor into other parts of the brain. It is therefore important to predict the migration pattern of the invasive cells; such detailed predictions are not known at this time. The migration of tumor cells from the primary tumor depends both on the tumor cell line and on the tumor microenvironment. Experimental results show various migration patterns of glioma, including isolated islands, branching, and dispersion near the tumor boundary as well as at some distance from the primary tumor. Some patterns of glioma cell migration seen in experiments are shown in Figure 11. Figures 11(b) and 11(d) show branching pattern whereas frame (a) shows a pattern of dispersion; (c) is a somewhat intermediate case between branching and dispersion. Sander and Deisboeck [12], Khain and Sander [4] and Stein *et al.* [14] developed mathematical models, based on PDEs, in attempts to capture such migration patterns. There is also some

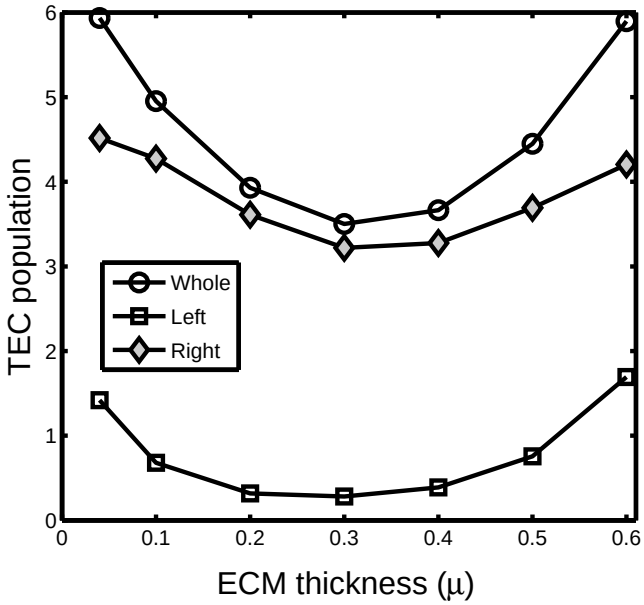

FIGURE 8. Effect of ECM coating (μ) on growth of TECs: Total population of TECs at day 4 in whole (circle), left (square), and right (filled diamond) chamber. The population of TECs has minimum values for the intermediate values of ECM thickness (μ).

work based on a single diffusion equation with coefficients that depend on geometric and physical features of the brain [15, 16].

Here we report on recent work by Kim *et al.* [7] which includes the chemotactic and haptotactic forces as well as cell-to-cell adhesion. The source of chemotaxis is glucose gradient and the source of haptotaxis is ECM gradient which is affected by MMPs produced by the tumor cells.

The model consists of a system of PDEs for the following variables: density of glioma cells and concentrations of ECM, MMP and nutrients (glucose). The model assumes that glioma cells shed off from the surface of the tumor, and tracks down the density of the cells for a period of time, for any particular choice of the following three parameters: chemotactic sensitivity (χ_n) of cells moving in the direction of the gradient of glucose, haptotactic sensitivity (χ_n^1) of cells moving in the direction of gradient of ECM concentration, and cell-cell adhesion force λ_a. Shedding of tumor cells from the spherical tumor occurs at random times from random locations. By 'somewhat' regularizing the shedding, we simulated the model in the cases of annular and rectangular geometry. Figure 12 is a simulation of the model for a simple rectangular geometry for different choices of χ_n^1 and λ_a. It shows patterns of branching, dispersion, and mixtures of the two.

We can use the model to develop testable hypotheses for slowing down glioma cells migration. One hypothesis is that increase in cell-cell adhesion will slow down tumor migration. This, in fact, is also suggested by experiments conducted *in vitro* and *in vivo* by Asano *et al.* [1]. Another way to slow migration is by blocking the

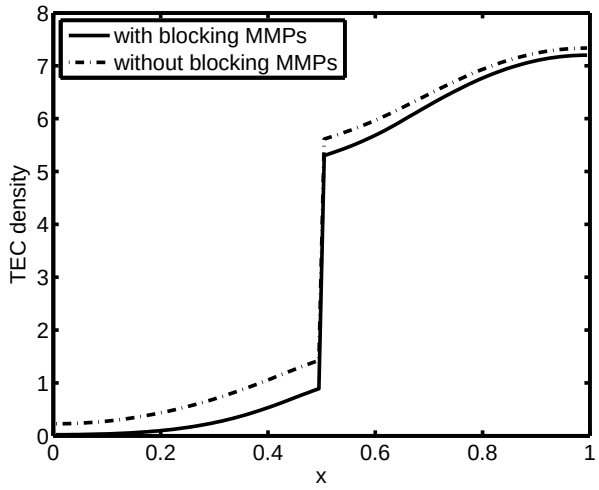

FIGURE 9. The growth of the TEC population where ECM degradation term is zero in comparison with its growth when MMP is not blocked. When proteolytic activity of TECs near membrane via MMPs is blocked, less cells are invading the left chamber. The filter is placed at x = 0.5.

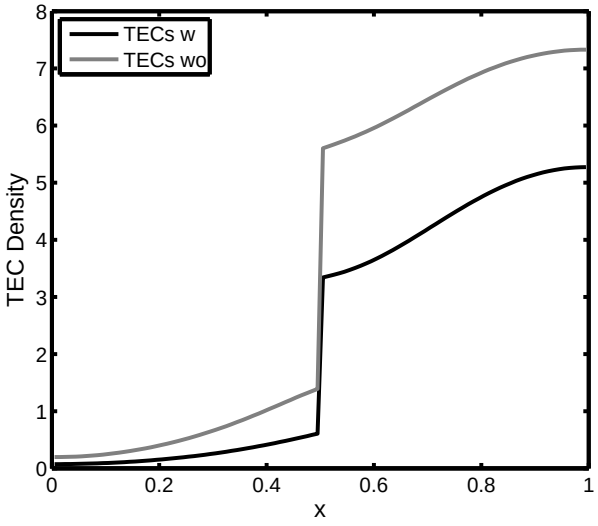

FIGURE 10. The growth of the TEC population at day 4 when TGF-β production is blocked or not blocked. Profile of TECs on domain x with (w) and without (wo) blocking TGF-β pathway.

effect of MMP, which can be achieved, for example, by viral transduction of siRNA, or some chemical inhibitors. We note that blocking the activity of MMP in order

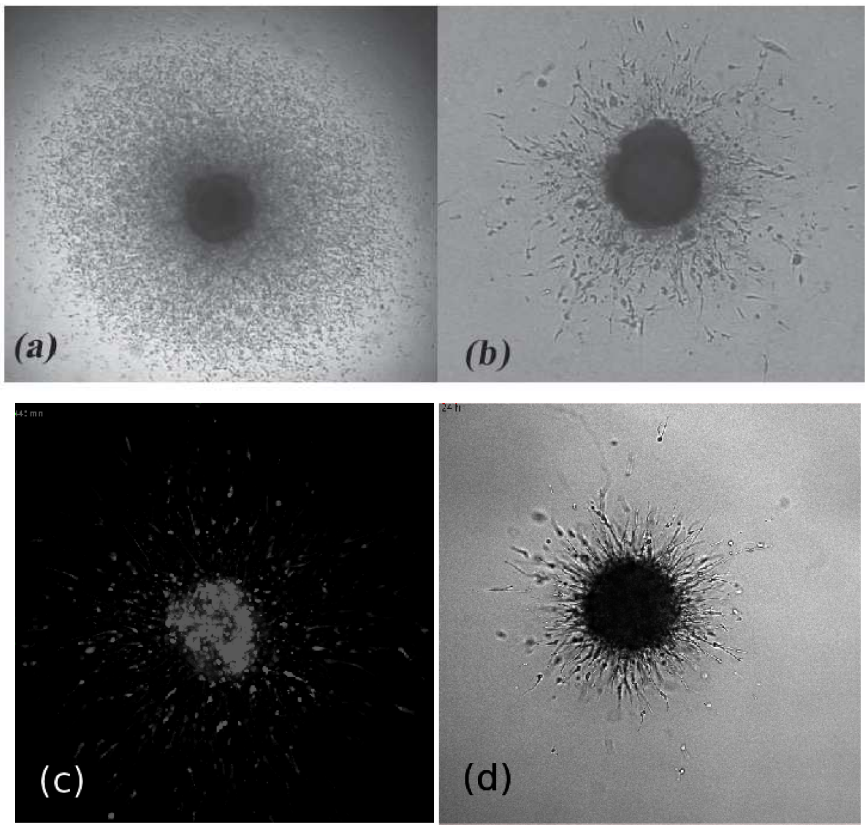

FIGURE 11. The four figures are taken from *in vitro* experiments with four different glioma lines: (a) U87, (b) U87ΔEGFR (a mutant of U87); (c) U87STM (d) X12RFP All cells shown were implanted into a type I collagen matrix and grown in DMEM containing 10% fetal calf serum and 4.5 $g/liter$ glucose. Figures 11(a) and 11(b) were reprinted with permission from E. Khain and L.M. Sander, Dynamics and pattern formation in invasive tumor growth, Phys Rev Lett, 96, 188103 (2006). Copyright(2006) by the American Physical Society. Figure 11(c)-(d) are replicated from experiments conducted by the co-authors Sean Lawler, Michal O. Nowicki of [17] in E. Antonio Chiocca's lab.

to slow tumor proliferation and migration was also suggested by the simulations in Section 2.

The model in [7] assumes that the tumor is spherical and that its microenvironment is initially homogeneous. However any inhomogeneities, which occur naturally in the brain, may result in significant changes in the pattern of cell migration. Modeling of migration patterns in the presence of such inhomogeneities remains an interesting and important problem.

All the simulations in Sections 1-3 were performed using a finite volume method and clawpack (http://www.amath.washington.edu/~claw/) with fractional step method as well as the non-linear solver *nksol* for algebraic systems.

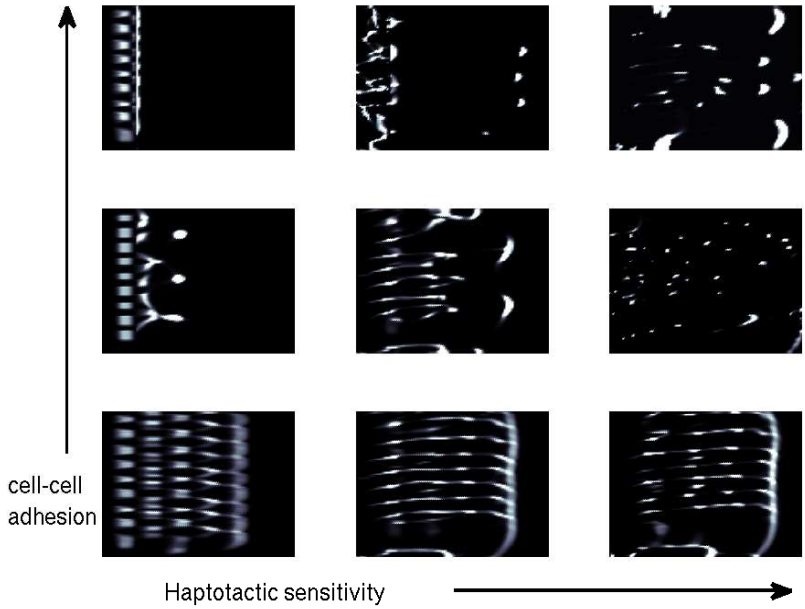

FIGURE 12. Effect of cell-cell adhesion (λ_a) and haptotactic sensitivity (χ_n^1) at a terminal time T. Cells are shedded from the left side of the frames in the first column. As cell-cell adhesion increases, migration is slowed down and, as it decreases, branching patterns appear.

4. **Discussion and conclusions.** Tumor cells proliferation and migration depend on the type of tumor cells and on the tumor microenvironment. In this review we focused on tumor epithelial cells (TECs) from breast cancer, and on tumor cells from glioblastoma. TGF-β is a major chemokine elevated in breast cancer, which increases tumor cells proliferation, survival and metastasis. It is promoted by EGF secreted by fibroblasts and myofibroblasts. To explore the mutual interaction between TGF-β and EGF we reported in Section 1 on our work[6] in which we developed a novel model and verified a key prediction of the model experimentally. Since the model was based on indirect interactions between cells separated by a permeable membrane, our model probably best describe the initial evolution of breast cancer, when the tumor cells are still confined to the mammary duct. Our study may thus lead to new concepts useful for understanding and eventually targeting the early stages of cancer development.

In Section 2 we reported on further development of the model in Section 1, using the setup of Boyden Invasion Chamber. We have drawn a number of conclusions, some of which agree qualitatively with experimental results, while others that we have stated as hypotheses to be tested experimentally. One of the interesting hypotheses suggested by our simulations is that as the thickness μ of the ECM layer increases the total TEC population decreases as long as $\mu < \mu_0$ and then it increases for $\mu > \mu_0$. This may be explained by "competition for space" which is undergoing within the ECM layer located between the TEC and the fibroblasts/myofibroblasts.

In Section 3 we reported on our work[7] which deals with migration patterns of glioma cancer cells shedded from primary spherical tumor. We determined, by simulation, how the forces of chemotaxis, haptotaxis and cell adhesion affect the migration pattern. The simulations suggest some biologically testable hypotheses for slowing down glioma cell migration. In particular, increased cell-to-cell adhesion between glioma cells could act to prevent single cells migration away from the primary tumor. Blocking the effect of MMP can also slow down cell migration. Although both conclusions seem "reasonable" the advantage of the mathematical model is in quantifying these statements.

Acknowledgments. We would like to thank the referees very much for their valuable comments and suggestions.

REFERENCES

[1] K. Asano, C. D. Duntsch, Q. Zhou, J. D. Weimar, D. Bordelon, J. H. Robertson and T. Pourmotabbed, *Correlation of n-cadherin expression in high grade gliomas with tissue invasion*, J Neurooncol, **70** (2004), 3–15.

[2] S. Aznavoorian, M. L. Stracke, H. Krutzsch, E. Schiffmann and L. A. Liotta, *Signal transduction for chemotaxis and haptotaxis by matrix molecules in tumor cells*, J Cell Biol, **110** (1990), 1427–38.

[3] N. A. Bhowmick, E. G. Neilson and H. L. Moses, *Stromal fibroblasts in cancer initiation and progression*, Nature, **432** (2004), 332–7.

[4] E. Khain and L. M. Sander, *Dynamics and pattern formation in invasive tumor growth*, Phys. Rev. Lett., **96** (2006), 188103.

[5] Y. Kim and A. Friedman, *Interaction of tumor with its microenvironment: A mathematical model*, Bull. Math. Biol., **72** (2010), 1029–1068.

[6] Y. Kim, J. Wallace, F. Li, M. Ostrowski and A. Friedman, *Transformed epithelial cells and fibroblasts/myofibroblasts interaction in breast tumor: A mathematical model and experiments*, J. Math. Biol., **61** (2010), 401–421.

[7] Y. Kim, S. Lawler, M. O. Nowicki, E. A Chiocca and A. Friedman, *A mathematical model of brain tumor : Pattern formation of glioma cells outside the tumor spheroid core*, Journal of Theoretical Biology, **260** (2009), 359–371.

[8] G. Lolas, *Mathematical modelling of proteolysis and cancer cell invasion of tissue*, in "Tutorials in Mathematical Biosciences III," Springer Berlin/Heidelberg, (2006), 77–129.

[9] M. M. Mueller and N. E. Fusenig, *Friends or foes - bipolar effects of the tumour stroma in cancer*, Nat Rev Cancer, **4** (2004), 839–49.

[10] A. J. Perumpanani and H. M. Byrne, *Extracellular matrix concentration exerts selection pressure on invasive cells*, Eur. J. Cancer, **35** (1999), 1274–80.

[11] M. Samoszuk, J. Tan and G. Chorn, *Clonogenic growth of human breast cancer cells co-cultured in direct contact with serum-activated fibroblasts*, Breast Cancer Res, **7** (2005), R274–R283.

[12] L. M. Sander and T. S. Deisboeck, *Growth patterns of microscopic brain tumors*, Phys. Rev. E, **66** (2002), 051901.

[13] J. A. Sherratt and J. D. Murray, *Models of epidermal wound healing*, Proc. R. Soc. Lond., **B241** (1990), 29–36.

[14] A. M. Stein, T. Demuth, D. Mobley, M. Berens and L. M. Sander, *A mathematical model of glioblastoma tumor spheroid invasion in a three-dimensional in vitro experiment*, Biophys. J., **92** (2007), 356–65.

[15] K. R. Swanson, E. C. Alvord and J. D. Murray, *A quantitative model for differential motility of gliomas in grey and white matter*, Cell Prolif., **33** (2000), 317–29.

[16] K. R. Swanson, E. C. Alvord and J. D. Murray, *Virtual resection of gliomas: Effect of extent of resection on recurrence*, Math. Comp. Modelling, **37** (2003), 1177–1190.

[17] M. Yashiro, K. Ikeda, M. Tendo, T. Ishikawa and K. Hirakawa, *Effect of organ-specific fibroblasts on proliferation and differentiation of breast cancer cells*, Breast Cancer Res Treat, **90** (2005), 307–13.

[18] K. Yuan, R. K. Singh, G. Rezonzew and G. P. Siegal, *Cell motility in cancer invasion and metastasis*, in "Cancer Metastasis - Biology and Treatment," Springer, Netherlands, (2006), 25–54.

Received February 2, 2010; Accepted October 30, 2010.

E-mail address: afriedman@math.osu.edu
E-mail address: yangjink@umd.umich.edu